

Title: Influence of hydrodynamics and nutrients on biofilm structure.

Running title: Biofilm structures.

Authors: P. Stoodley^{1*}, I. Dodds², J.D.Boyle², and H.M. Lappin-Scott¹

1 Environmental Microbiology Research Group - Exeter University

Hatherly Laboratories, Prince of Wales Road.

Exeter EX4 4PS. UK.

2 School of Engineering

North Park Road,

Exeter University,

Exeter EX4 4QF. UK.

Stoodley, P., Dodds, I., Boyle, J.D., and Lappin-Scott, H.M. 1999. Influence of hydrodynamics and nutrients on biofilm structure. *J. Appl. Microbiol.* **85**:19S-28S.

Accession No: 6667/4/98

Corresponding author:

Paul Stoodley

Environmental Microbiology Research Group - Exeter University (EMRGE)

Hatherly Laboratories, Prince of Wales Road, Exeter EX4 4PS. UK.

Tel: 01392 264348, Fax: 01392 263700, email: p.stoodley@exeter.ac.uk

1. **SUMMARY**
2. **INTRODUCTION**
3. **MATERIALS AND METHODS**
 - 3.1 **Biofilm Reactor System**
 - 3.2 **Reactor sterilisation**
 - 3.3 **Inoculum**
 - 3.4 **Species identification and enumeration**
 - 3.5 **Nutrients**
 - 3.6 **Experimental runs**
 - 3.7 **Microscopy and image analysis**
 - 3.8 **Surface concentration of cells and cell clusters**
 - 3.9 **Cell cluster thickness measurements**
 - 3.10 **Percent surface coverage and cell cluster dimensions**
 - 3.11 **Enumeration of viable biofilm bacteria**
 - 3.12 **Statistical Analysis**
4. **RESULTS**
 - 4.1 **Run 1 - effect of flow on biofilm development and morphology**
 - 4.1.1 *Suspended and biofilm populations*
 - 4.1.2 *Biofilm morphology*
 - 4.1.3 *Biofilm surface coverage*
 - 4.2 **Run 2 - effect of nutrient changes on biofilm grown in turbulent flow**
 - 4.2.1 *Suspended and biofilm populations*
 - 4.2.2 *Biofilm morphology*
5. **DISCUSSION**
 - 5.1 **Influence of flow on biofilm development and morphology at low nutrient concentration**
 - 5.2 **Influence of changing nutrients on the structure of biofilm grown in turbulent flow**
 - 5.3 **Biofilm morphotypes and habitat domains**
 - 5.4 **Quantification of biofilm structure**
6. **ACKNOWLEDGEMENTS**
7. **REFERENCES**

1. SUMMARY

Hydrodynamic conditions control two interlinked parameters; mass transfer and drag, and will, therefore, significantly influence many of the processes involved in biofilm development. The goal of this research was to determine the effect of flow velocity and nutrients on biofilm structure. Biofilms were grown in square glass capillary flow cells under laminar and turbulent flows. Biofilms were observed microscopically under flow conditions using image analysis. Mixed species bacterial biofilms were grown with glucose (40 mg/l) as the limiting nutrient. Biofilms grown under laminar conditions were patchy and consisted of roughly circular cell clusters separated by interstitial voids. Biofilms in the turbulent flow cell were also patchy but these biofilms consisted of patches of ripples and elongated “streamers” which oscillated in the flow. To assess the influence of changing nutrient conditions on biofilm structure the glucose concentration was increased from 40 to 400 mg/l on an established 21 day old biofilm growing in turbulent flow. The cell clusters grew rapidly and the thickness of the biofilm increased from 30 μm to 130 μm within 17 h. The ripples disappeared after 10 hours. After 5 d the glucose concentration was reduced back to 40 mg/l. There was a loss of biomass and patches of ripples were re-established within a further 2 d.

2. INTRODUCTION

In recent years there has been a shift in our perception of the structure of bacterial biofilms from that of an homogenous layer of cells in a slime matrix to a much more heterogenous arrangement. This shift was facilitated mainly by the use of flow cells and the application of confocal microscopy to observe fully hydrated biofilms at high resolution. Much of the pioneering work was done by Caldwell and colleagues in the late 1980's and early 1990's (Lawrence *et al.* 1991; Caldwell *et al.* 1993). It has been widely reported that biofilms consist of clumps of cells separated by interstitial voids and channels (deBeer *et al.* 1994a; Massol-Deya *et al.* 1994; Moller *et al.* 1998). Further, it was discovered that water could flow through the channels (Stoodley *et al.* 1994) and facilitate the mass transfer of nutrients to biofilm bacteria (deBeer and Stoodley 1995; deBeer *et al.* 1996). In addition to mass (and heat) transfer, biofilm structure will also influence drag in a flowing system, which in turn may effect detachment (Kwok *et al.* 1998) and energy losses (Lewandowski and Stoodley 1995; Stoodley *et al.* 1998, 1999). Knowledge of biofilm structure allows a better understanding of how developing biofilms are influenced by the surrounding environment and affords us better interpretation of biofilm processes; both of which are important if we are to more effectively utilise and control biofilms in industrial and medical settings.

Two important factors which can influence the structure of biofilms growing in aqueous environments are flow velocity and nutrient status. The flow velocity determines the hydrodynamic shear and the mass transfer characteristics of a system. It has been established that (steady state) biofilm thickness increases with nutrient concentration when shear is held constant (Characklis 1990) but decreases with shear when the substrate loading rate is constant (Characklis 1981). The relationship order

between thickness and shear is proportional to substrate loading rate and approaches zero order for low substrate loading (Characklis 1981). Lewandowski and Walser (1991) found that the thickness of a mixed culture biofilm was at a maximum near the transition between laminar and turbulent flows. They hypothesised that there was an optimal Reynolds number below which accumulation was mass transfer limited and above which accumulation was limited by shear induced detachment. Although there are data on the effects of nutrients and shear on the physical characteristics of biofilm (such as thickness, mass, and density) there is relatively little comparative data on biofilm morphology (van Loosdrecht *et al.* 1995). For planar biofilms spatially averaged physical parameters are enough to describe and model biofilm processes, but are not adequate for heterogenous biofilms, for which morphology at the micro scale will determine important factors such as porosity, surface exchange area, and drag related frictional losses.

It was the goal of this study to document, and quantify, the influence of hydrodynamics and changing nutrient status on the development and structure of a mixed species biofilm using in situ microscopic monitoring and image analysis.

3. MATERIALS AND METHODS

3.1 Biofilm Reactor System

The reactor system consisted of two flow cells which were incorporated into a recycle loop with a mixing chamber for aeration and nutrient addition (Fig. 1). The flow cells were 20 cm lengths of 3x3 mm square glass tubing (S-103 Camlab Ltd., Cambridge, UK.) which were cut from stock using a diamond knife. Nutrients were delivered by peristaltic pump (Masterflex, Cole Parmer, Niles, IL, USA) and the recycle flow rate was controlled with a vane head pump (Masterflex, Cole Parmer, Niles, IL, USA). The volume (V) of the mixing chamber and recycle loop, including the flow cells, was 175 ml. The nutrient influent flow rate (Q_n) was 4.3 ml/min giving a resulting residence time ($q = V/Q_n$) in the entire system of 40 minutes. The flow velocity through each of the flow cells (u) was controlled independently by tightening or loosening clamps on the inlet tubing and measured using flow meters (McMillan Flo-sensor model 101T # 3724 and 3835 supplied by Cole-Parmer, Niles, IL). The flow velocity in one flow cell was maintained at $u = 0.033$ m/s (Reynolds number, Re , 120) and in the other was 1.0 m/s (Re 3600). At these velocities flow was laminar in the former and turbulent in the latter, the transition point being at Re 1200 (Stoodley *et al.* 1998). The flow cells were positioned on a polycarbonate holder which was mounted on the stage of an Olympus BH2 upright microscope. The biofilm could be imaged *in situ* without interrupting flow. A septum sealed sampling port was positioned between two flow breaks in the effluent line.

Under operating conditions the water temperature in the reactor system was 28°C and all experiments were performed at this temperature.

3.2 Reactor sterilisation

The reactor system and nutrients were sterilised by autoclaving at 121°C for 15 minutes. The flow meter was sterilised using a method adapted from Fisher and Petrini (1992) in which it was exposed to 70 % ethanol for 15 minutes, 40% NaOCl solution (approx. 12% available chlorine when undiluted) for 15 minutes, and 70 % ethanol for 15 minutes. To check for sterility the flow system was operated with sterile media for 3 days prior to inoculation. Sterility was confirmed by plating three 0.1 ml aliquot effluent samples onto King's B agar (King *et al.* 1954).

3.3 Inoculum

Four gram negative species, *Pseudomonas aeruginosa* (ERC1), *Pseudomonas fluorescens*, *Klebsiella pneumoniae* and *Stenotrophomonas maltophilia*, commonly isolated from environmental and industrial biofilms were used to inoculate the reactor. *P. aeruginosa* (ERC1) was an environmental isolate, and *P. fluorescens* and *K. pneumoniae* were laboratory isolates (Stoodley *et al.* 1994). *S. maltophilia* was isolated from an undefined laboratory culture and identified using the Biolog system (similarity index = 0.706 after 24 hr, Biolog Inc., Hayward, CA.) and fatty acid analysis (similarity index = 0.727, MIDI, Newark, DE.). Frozen stock cultures (0.5 ml of 3×10^8 to 4×10^9 CFU/ml) of each of the species were thawed and injected directly into the mixing chamber. The time of inoculation was taken as the zero time point. The reactor was initially run as a recirculating batch culture for 24 hours, before switching to continuous culture. Effluent samples were taken periodically to monitor the suspended population.

3.4 Species identification and enumeration

Each of the four species could be identified and enumerated by serial plating on King's B agar with added brom-thymol blue (BTB, 0.03 g/l) as a pH indicator. *K. pneumoniae* formed large, smooth, yellow (from acid production) colonies, *P. fluorescens* formed strongly fluorescent large cream colonies with an undulate margin, *P. aeruginosa* formed weakly fluorescent small bluish green rough colonies, and *S. maltophilia* formed small, smooth, green colonies. Because the species appeared in different numbers on the plates various dilutions were counted. CFUs on the lower dilution plates were identified and counted after 24 hours with a dissecting microscope to minimise the problem of the more numerous species crowding out the others. Using this method individual species could be detected in numbers down to approximately 0.5% of the total population.

3.5 Nutrients

Two minimal salts growth media were used. Low nutrient media: glucose (40 mg/l), $(\text{NH}_4)_2\text{SO}_4$ (10 mg/l), KH_2PO_4 (70 mg/l), K_2HPO_4 (30 mg/l), $\text{MgSO}_4 \cdot 7\text{H}_2\text{O}$ (10 mg/l) and trace elements: $\text{Na}_2\text{EDTA} \cdot 2\text{H}_2\text{O}$ (12 mg/l); $\text{FeSO}_4 \cdot 7\text{H}_2\text{O}$ (2 mg/l); CaCl_2 (1 mg/l); Na_2SO_4 (1 mg/l), $\text{ZnSO}_4 \cdot 7\text{H}_2\text{O}$ (4 mg/l); $\text{MnSO}_4 \cdot 4\text{H}_2\text{O}$ (4 mg/l); $\text{CuSO}_4 \cdot 5\text{H}_2\text{O}$ (1 mg/l); $\text{Na}_2\text{MoO}_4 \cdot 2\text{H}_2\text{O}$ (1 mg/l). High nutrient media: glucose (400 mg/l), $(\text{NH}_4)_2\text{SO}_4$ (100 mg/l), otherwise the same. The media was sterilised by autoclaving at 121°C with an exposure time of 15 minutes. The final pH was 6.8. Dissolved oxygen (DO) was monitored periodically by a colorimetric method using R-7501 CHEMets ampoules (CHEMetrics Inc., Calverton, VA.). The DO concentration in the effluent did not fall below 1 mg/l.

3.6 Experimental runs

Two experimental runs, Run 1 and Run 2, were performed. For Run 1, biofilms were grown in both laminar and turbulent flows for 23 days on low nutrient medium only. For the second run only the turbulent flow cell was used. The biofilm was grown on low nutrient medium for the first 21 days, high nutrient medium for the next 5 days (days 22-26), and low nutrient medium for the remaining 3 days of the experiment (days 26-29).

3.7 Microscopy and image analysis

The biofilm was observed using transmitted light and a range of Olympus objectives from 4X to 100X. A COHU 4612-5000 CCD camera (Cohu, Inc., San Diego, CA. USA) and a Scion VG-5 PCI framestore board (Scion Inc. Frederick, MD. USA) were used to capture images. Image processing was done on a Macintosh 7200/90 computer using the public domain NIH-Image 1.59 program (developed at the National institutes of Health and available from the Internet by anonymous FTP from zippy.nimh.nih.gov or a floppy disk from the National Technical information service, Springfield, Virginia, USA, part number PB95-500195GEI). A 1mm graticule with 10 μm divisions (Ref. # CS990, Graticules Ltd., Tonbridge, Kent, UK) was used for calibration.

3.8 Surface concentration of cells and cell clusters

The surface concentration of single cells and cell clusters were measured in the laminar and turbulent flow cells on day nine. Single cells in the base film between clusters were counted in three $2407 \mu\text{m}^2$ fields using a 100X objective. Cell clusters were counted in ten 1.036 mm^2 fields using a 4X objective. The 4X objective was used so that the complete width of the flow cell could be imaged, thus giving more

representative sampling, however, we estimated that only clusters with diameters greater than 10 μm were included in the count.

3.9 Cell cluster thickness measurements

The thickness of the largest biofilm cell clusters (l_c) were periodically measured microscopically using a 40X objective by focusing on the glass substratum and then moving the stage a known distance (using the scale on the focus knob) until the top surface of the cell cluster came into focus. The “apparent” thickness was multiplied by a correction factor of 1.36 to find the actual thickness (Stoodley *et al.* 1997). Each measurement was averaged from a minimum of five cell clusters.

3.10 Percent surface coverage and cell cluster dimensions

Biofilm surface coverage was periodically measured in the laminar and turbulent flow cells. Five 11107 μm^2 fields of view (using a 40X objective) were captured and a threshold applied so that the biofilm features were black and the surrounding voids and channels white. The relative surface coverage of the biofilm was the proportion of black to the total area.

The length to width ratio (l:w) of biofilm cell clusters growing in the laminar and turbulent flows was used as an indicator of shape difference caused by the different flows. The cluster width, for this study, is defined as the dimension perpendicular to the flow direction (parallel with the substratum), and was measured at the widest point on the cluster. The length was parallel with the flow direction. Biofilms were imaged with a 4X objective and measurements made using the “line tool” function..

3.11 Enumeration of viable biofilm bacteria

At the end of the experiments, the flow cells were removed from the reactor and rinsed 5 times with 1 ml sterile buffer ($1/4$ strength Ringers soln.). The flow cells were sectioned with a diamond knife and immersed in 5 ml sterile buffer with 0.1% (w/v) Tween 20. Samples were sonicated for 3 x 5 minutes and vortexed between sonications for 10 seconds. Microscopic examination of the sections before and after sonication showed that the surface area covered by biofilm was reduced by 98.2%, as measured by image analysis. The proportion of recovered biomass was probably higher than this since the remaining biofilm was at most a few cell layers thick, including the corners of the flow cell. Serial dilutions were plated onto King's B + BTB agar. Plates were incubated at 24°C and counted after 48 hours.

3.12 Statistical Analysis

Where data means are given, the standard error (SE) associated with the mean and sample number (n) are also indicated. Statistical comparisons were done by one way analysis of variance (ANOVA) using Quattro Pro 6.0 (Novell Inc.) and differences reported significant at the 5% level.

4. RESULTS

4.1 Run 1 - effect of flow on biofilm development and morphology

4.1.1 *Suspended and biofilm populations*

The suspended population stabilised after approximately 10 days and at 23 days the relative proportions of species in the effluent were similar to those in the biofilms (Table 1)

4.1.2 *Biofilm morphology*

After nine days the biofilm in the laminar flow cell was heterogenous and consisted of cell clusters separated by interstitial voids. The clusters were roughly circular in shape and up to 100 μm in diameter (Fig. 2). There were 5.1×10^2 clusters/ cm^2 (standard error, $\text{SE}=0.53 \times 10^2$, $n=10$). In the void areas there was a sparse covering of single cells (8.5×10^6 cells/ cm^2 , $\text{SE}=0.26 \times 10^6$, $n=3$). The biofilm in the turbulent flow was also heterogenous but in addition to cell clusters, ripple-like structures were present. The clusters were tapered in the downstream direction forming streamers. The streamers were up to 700 μm in length and 370 μm in width (Fig. 2). Some of the streamers were free to oscillate in the flow stream and others were more firmly attached to the substratum. The surface concentration of clusters was 7.9×10^2 clusters/ cm^2 ($\text{SE}=0.56 \times 10^2$, $n=10$). In the voids there were 5.8×10^6 cells/ cm^2 ($\text{SE}=0.20 \times 10^6$, $n=3$). After 23 days the clusters in the laminar flow cell were relatively unchanged, while those in the turbulent flow cell had elongated up to 1200 μm (Fig. 2). There was no significant difference between the thickness of clusters in the laminar (58 μm , $\text{SE}=5$, $n=5$) and turbulent (41 μm , $\text{SE}=13$, $n=5$) flow cells. The biofilms at 22 days are shown in Figs. 3A and B. The l:w ratio was used to demonstrate the influence of flow on the shape of the cell clusters over time (Fig. 4).

The l:w ratio for the clusters in the laminar flow increased from 1.08 (SE=0.04, n=7) at day eight to 1.78 (SE=0.12, n=33) at day 23, while in the turbulent flow the l:w ratio increased from 2.18 (SE=0.12, n=7) to 7.61 (SE=1.30, n=24) over the same period.

4.1.3 *Biofilm surface coverage*

The progression of surface coverage of biofilm in the flow cells is shown in Fig. 5. Surface coverage of the laminar flow cell increased at rate of 10% per day for the first six days, 2.4 times the rate in the turbulent flow cell (4%/day). Coverage reached a plateau value of approximately 60% after six days. In the turbulent flow cell a plateau value of approximately 80% was reached after 13 days.

4.2 **Run 2 - effect of nutrient changes on biofilm grown in turbulent flow**

4.2.1 *Suspended and biofilm populations*

The suspended populations for the first 21 days were similar to those in Run 1 and after 10 days the species concentrations were relatively stable with *K. pneumoniae* as the dominant organism (ca. 2×10^7 CFU/ml, 80%) and *P. aeruginosa* the second most abundant (ca. 3×10^6 CFU/ml, 10%). Two days after switching to the high nutrients the concentrations of each of the four species had increased by approximately a factor of 20 so that the proportions remained essentially constant (Fig. 6). The populations remained stable for the next three days until the medium was switched back to the low nutrients (day 26). The concentration of each species then fell and by day 29 were similar to those values at day 21.

4.2.2 *Biofilm morphology*

After 18 days the biofilm was similar to that grown in Run 1 and consisted of cell clusters, streamers and patches of ripples. The thickness of the cell clusters was 13 μm (SE=1.3, n=9) (Fig. 7). At day 20 there was little change in the appearance of the biofilm but the thickness of the cell clusters had increased to 26 μm (SE=2.6, n=7). At day 21 the biofilm was unchanged and there was no significant difference in the thickness of the cell clusters (26 μm (SE=2.7, n=5) (Fig. 8A). The surface coverage of the biofilm was 52.2 % (SE=5.9, n=5) (Fig. 7). Ten hours after switching to the high nutrient media the cell clusters and streamers had grown much larger and the ripples had disappeared (Fig. 8B). At day 22 the thickness of the cell clusters and the surface coverage had increased to 130 μm (SE=6.9, n=5) and 91.2% (SE=3.8, n=5) respectively. Many of the cell clusters had merged together and the streamers were difficult to distinguish. The appearance of the biofilm did not noticeably change up to day 26 (Fig. 8C) although the thickness of the cell clusters and the surface coverage had reduced to 83 μm (SE=9.4, n=5) and 80.8% (SE=8.1, n=5) respectively. After the media was switched back to the low nutrients there was an immediate net loss of biomass and after 2 days (day 28) the ripple patches and streamers had reappeared (Fig. 8D).

5. DISCUSSION

5.1 Influence of flow on biofilm development and morphology at low nutrient concentration

The morphology of the biofilms grown in laminar and turbulent flows were markedly different. Since the species proportions were similar in both biofilms such differences may be explained by difference in mass transfer and shear characteristics caused by the different flow regimes.

Biofilm accumulation, measured by surface coverage (Fig. 5), of both the laminar and turbulent flow cells followed a sigmoidal progression similar to that reported using measurements of thickness or mass (Bryers and Characklis 1981). The biofilm growing in laminar flow colonised the glass surface at a greater rate than the biofilm in turbulent flow but reached steady state earlier (Fig. 5). The steady state coverage was lower for the laminar flow cell. This observation may be explained by the influence of flow velocity on attachment, growth, and detachment. A mass balance equation for biofilm accumulation can be written as; accumulation rate = attachment rate + growth rate - detachment rate (Bryers and Characklis 1981). Growth and detachment will normally increase as a function of flow velocity, in the case of growth because of increased mass transfer, and in the case of detachment because of increased shear. For attachment, faster flow will bring more cells into contact with the surface due to better mixing but the sticking efficiency may be reduced because of higher shear. It is possible that in the laminar flow cell accumulation rate was higher because the detachment rate was relatively low with respect to growth rate but steady state was reached sooner because of nutrient transfer limitations.

For thin biofilms accumulation can be estimated by surface coverage, but for thicker biofilms thickness measurements are also required for better estimation. In this study we measured the thickness of the larger cell clusters at the thickest point. Dependant on surface distribution, generally it will be the thicker cell clusters that determine frictional energy losses. An alternative approach is that of Moller *et al.* (1997) who measured thickness at random locations so that both cell clusters and voids were included in the sampling, thus giving an average biofilm thickness. Microscopically, thickness measurements are simple but since, with conventional equipment, are manual, collecting a representative sample may be time consuming and difficult to perform non-subjectively. Another problem with the use of microscopic techniques for biomass estimation is that flow cell edges and inlet and outlet regions are difficult and often impossible to sample.

The morphology of biofilm features in the turbulent flow cell revealed the influence of hydrodynamic drag. The clusters became progressively elongated over time to form streamers (Fig. 4). Similar structures have been previously reported in turbulent flows and have been implicated with increased frictional energy losses in water pipelines (Bryers and Characklis 1981; McCoy *et al.* 1981; Picaloglou *et al.* 1980; Stoodley *et al.* 1998, 1999) . It is expected that, at high shear, as cells divide the drag force will tend to push daughter cells in the downstream direction, redepositing cells from the leading edge to the wake region at the trailing edge (Lewandowski and Stoodley 1995). The formation of transverse ripples is also suggestive of surface transport, a drag related phenomenon. In both flow cells bacteria were observed moving over the surface although in the turbulent flow cell downstream movement was much more evident. Gjaltema *et al.* (1994) have previously reported similar “dune” structures in pure culture *P. aeruginosa* biofilms growing in turbulent flow.

5.2 Influence of changing nutrients on the structure of biofilm grown in turbulent flow

When the limiting nutrients, carbon and nitrogen, were increased by a factor of ten the biofilm responded immediately. In addition to an increase in biomass (indicated by increased biofilm thickness and surface coverage, Fig. 7) the biofilm also changed morphologically. The ripples disappeared and the clusters and streamers grew larger, many of them merging, to form a porous structure. The influence of drag on the biofilm was much less evident (Fig 8c). As the biofilm increased in thickness and surface area coverage it is possible that the flow regime switched from “isolated roughness” or “wake interaction flow” to “skimming flow” (Nowell and Church, 1979). When surface protrusions (such as biofilm clusters) cover only a small proportion of the surface an “isolated roughness flow” may occur in which each cluster experiences essentially the same shear forces. When cell clusters are closer together wakes shed from upstream clusters may not dissipate before interacting with downstream clusters resulting in “wake interaction flow”. In this case the shear rate in the voids will be lower than for a smooth surface. deBeer *et al.* (1994b) reported that the velocity gradient, and therefore, the shear rate in the voids of an heterogeneous biofilm were approximately 50% those at a clean surface indicating that “wake interaction” flow was occurring. At high surface cover a “skimming flow” may occur in which the velocity profile is vertically relocated to the top of the biofilm cell clusters. In this case although there may be some pressure driven convective flow through biofilm channels the shear rate in the voids will be greatly diminished. When the nutrients were decreased to the original levels there was a net loss of biomass and the ripples and streamers began to reform demonstrating that the changes in biofilm

morphology were reversible. It is possible that the loss of biomass caused changes in the flow regime resulting in increased local shear rate, and drag, in the void areas.

Most experiments concerned with the influence of environmental parameters on biofilm development compare biofilms grown under one set of conditions with those grown under another set of conditions. Although this approach allows clearer interpretation, the influence that changing environmental conditions have on established biofilms is arguably more relevant to many industrial and environmental systems.

5.3 Biofilm morphotypes and habitat domains

This work demonstrates that hydrodynamics and changing nutrient concentrations can have a significant impact on biofilm morphology. The biofilm was polymorphic and structurally adapted to changing nutrient conditions. The changes were reversible demonstrating that biofilm structure may be manipulated. The influence of particulates, corroding surfaces, predators, and natural consortia in uncontrolled “real” systems will add further levels of complexity. However, for some systems it may be possible to predict biofilm structure from nutrient and shear conditions as suggested by van Loosdrecht *et al.* (1995). Wimpenny (1996) used two dimensional habitat domains to illustrate how spatial or temporal changes in local environment may hypothetically influence microbial communities. It is possible to construct similar diagrams which predict biofilm morphotypes based on observational and theoretical considerations of the relative influences of nutrient concentration and shear. Such a diagram is shown in Fig. 9. At high shear, where the influence of drag is high but mass transfer limitations are low, we might expect drag reducing planar structures, the thickness of which depend on nutrient concentration. However, at low

shear, where the influence of mass transfer limitations are high but drag is low, we might expect highly porous structures with high surface exchange areas. Intermediate structures may occur elsewhere in the habitat domain. This type of diagram predicts that as environmental conditions change and move to new locations on the phase diagram biofilm morphology will respond accordingly and move towards a new equilibrium (steady state) position. Biofilm morphology in a changing environment at any point in time would, therefore, be dependant on the rate of change of conditions as well as the response rate of the biofilm. Changes in local conditions may be caused by the developing biofilm itself, in addition to those imposed by external influences.

5.4 Quantification of biofilm structure

Finally, if an understanding of biofilm morphology is necessary to explain and predict biofilm behaviour, as we believe it is, techniques must be developed which allow morphology to be quantified. Such parameters should be unambiguous so that a certain numerical value (or set of values) is unique to a particular morphology. At present fractal analysis shows the most promise (Hermanowicz *et al.* 1996; Zahid and Ganczarczyk 1994). However, fractal analysis, as with any image analysis can only be as good as the collected images which, even with sophisticated microscopy techniques, are very difficult to achieve with absolutely uniform staining and illumination throughout a 3D field.

6. ACKNOWLEDGEMENTS

This research was supported by the University of Exeter and in part by the co-operative agreement EEC-8907039 between the National Science Foundation and Montana State University - Bozeman. From the Department of Biological Sciences at Exeter University we thank Neville Barrett, Tony Davey, Stephen Forster, and Alan G. Hailey for their help with design and manufacture of the flow system.

7. REFERENCES

Bryers, J. and Characklis, W.G. (1981) Early fouling biofilm formation in a turbulent flow system: overall kinetics. *Water Research* **15**, 483-491.

Caldwell, D.E., Korber, D.R., and Lawrence, J.R. (1993) Analysis of biofilm formation using 2D vs 3D digital imaging. *Journal of Applied Bacteriology* **74**, pp.S52-S66.

Characklis, W.G. (1981) Fouling biofilm development: a process analysis. *Biotechnology and Bioengineering* **23**, 1923-1960.

Characklis, W.G. (1990) Microbial fouling. In *Biofilms* ed. Characklis, W.G. and Marshall, K.C. pp.523-584. Wiley, New York.

de Beer, D., P. Stoodley, F. Roe, and Z. Lewandowski (1994a) Effects of biofilm structures on oxygen distribution and mass transfer. *Biotechnology and Bioengineering* **43**, 1131-1138.

deBeer, D., Stoodley, P., and Lewandowski, Z. (1994b) Liquid flow in heterogenous biofilms. *Biotechnology and Bioengineering* **44**, 636-641.

deBeer, D. and Stoodley, P. (1995) Relation between the structure of an aerobic biofilm and mass transport phenomena. *Water Science and Technology* **32**, 11-18.

deBeer, D., Stoodley, P., and Lewandowski, Z. (1996) Liquid flow and mass transfer in heterogeneous biofilms. *Water Research* **30**, 2761-2765.

Fisher, P.J. and Petrini O. (1992) Fungal saprobes and pathogens as endophytes of rice (*Oryza sativa* L.). *New Phytologist* **120**, 137-143.

Gjaltema A., Arts P.A.M., van Loosdrecht M.C.M., Kuenen J.G., and Heijnen J.J. (1994) Heterogeneity of biofilms in rotating annular reactors: occurrence, structure, and consequences. *Biotechnology and Bioengineering* **44**, 194-204.

Hermanowicz, S.W., Schindler, U., and Wilderer, P. (1996) Anisotropic morphology and fractal dimensions of biofilms. *Water Research* **30**, 753-755.

King, O.E., Ward, M.K., and Raney, D.E. (1954) Two simple media for the demonstration of pyocyanin and fluorescein. *Journal of Laboratory and Clinical Medicine* **44**, 301-307.

Kwok, W.K., Picioreanu, C., Ong, S.L., van Loosdrecht, M.C.M., Ng, W.J., and Heijnen, J.J. (1998) Influence of biomass production and detachment forces on biofilm structures in a biofilm airlift suspension reactor. *Biotechnology and Bioengineering* **58**, 400-407.

Lawrence J.R., Korber D.R., Hoyle B.D., Costerton J.W., and Caldwell D.E. (1991) Optical sectioning of microbial biofilms. *Journal of Bacteriology* **173**, 6558-6567.

Lewandowski, Z. and Stoodley, P. (1995) Flow induced vibrations, drag force, and pressure drop in conduits covered with biofilm. *Water Science and Technology* **32**, 19-26.

Lewandowski, Z. and Walser, G. (1991) Influence of hydrodynamics on biofilm accumulation. In *Environmental Engineering Proceedings EE Div/ASCE, Reno, NV, July-8-10* pp. 619-624.

Massol-Deya A.A., Whallon J., Hickey R.F., and Tiedje J.M. (1994) Channel structures in aerobic biofilms of fixed-film reactors treating contaminated groundwater. *Applied and Environmental Microbiology* **61**, 769-777.

McCoy, W.F., Bryers, J.D., Robbins, J., and Costerton, J.W. (1981) Observations of fouling biofilm formation. *Canadian Journal of Microbiology* **27**, 910-917.

Møller, S., Korber, D.R., Wolfaardt, G.M., Molin, S., and Caldwell, D.E. (1997) Impact of nutrient composition on a degradative biofilm community. *Applied and Environmental Microbiology* **63**, 2432-2438.

Møller, S., Sternberg, C., Andersen, J.B., Christensen, B.B., Ramos, J.L., Givskov, M., and Molin, S. (1998) In situ gene expression in mixed-culture biofilms: evidence of metabolic interactions between community members. *Applied and Environmental Microbiology* **64**, 721-732.

Nowell, A.R.M. and Church, M. (1979) Turbulent flow in a depth limited boundary layer. *Journal of Geophysical Research, C: Oceans Atmos.* **84**, 4816-4824.

Picologlou, B.F., Zilver, N., and Characklis, W.G. (1980) Biofilm Growth and Hydraulic Performance. *Journal of the Hydraulics Division. American Society of Civil Engineers* **106**, No HY5 733-746.

Stoodley, P., deBeer, D. and Lewandowski, Z. (1994) Liquid flow in biofilm systems. *Appl. Environ. Microbiol.* **60**, 2711-2716.

Stoodley, P., Yang, S., Lappin-Scott, H.M, and Lewandowski, Z. (1997) Relationship between mass transfer coefficient and liquid flow velocity in heterogenous biofilms using microelectrodes and confocal microscopy. *Biotechnology and Bioengineering* **56**, 681-688.

Stoodley, P., Lewandowski, L., Boyle, J.D., and Lappin-Scott, H.M. (1998) Oscillation characteristics of biofilm streamers in turbulent flowing water as related to drag and pressure drop. *Biotechnology and Bioengineering* **57**, 536-544.

Stoodley, P., Boyle, J., Cunningham, A.B., Dodds, I., Lappin-Scott, H.M., and Lewandowski, Z. (1999) Biofilm structure and influence on biofouling under laminar and turbulent flows. In *Biofilms in Aquatic Systems*. eds. Keevil, C.S., Dow, A.F., Godfree A.F., and Holt, D. Cambridge: Royal Society of Chemistry. In press.

van Loosdrecht M.C.M., Eikelboom, D., Gjaltema, A., Mulder, A., Tjihuis, L. and Heijnen, J.J. (1995) Biofilm structures. *Water Science and Technology* **32**, 35-43.

Wimpenny, J. (1996) Ecological determinants of biofilm formation. *Biofouling*. **10**, 43-63.

Zahid, W. and Ganczarczyk, J. (1994) A technique for a characterization of RBC biofilm surface. *Water Research* **28**, 2229-2231.

TABLES

Table 1. Viable suspended and biofilm populations for Run 1 at day 23. The relative proportion of the individual species to the total population is shown as a percentage.

| Species | Suspended (CFU/ml) | Laminar biofilm (CFU/cm ²) | Turbulent biofilm (CFU/cm ²) |
|-----------------------|-----------------------------|---|---|
| <i>P. aeruginosa</i> | 1.6x10 ⁷ (22.2%) | 7.5x10 ⁶ (8.3%) | 4.0x10 ⁷ (11.9%) |
| <i>P. fluorescens</i> | 6.3x10 ⁵ (0.9%) | 1.1x10 ⁶ (1.2%) | 8.3x10 ⁶ (2.5%) |
| <i>K. pneumoniae</i> | 5.4x10 ⁷ (75.0%) | 7.8x10 ⁷ (87.0%) | 2.8x10 ⁸ (83.1%) |
| <i>S. maltophilia</i> | 1.4x10 ⁶ (1.9%) | 3.1x10 ⁶ (3.4%) | 8.3x10 ⁶ (2.5%) |
| Total | 2.2x10 ⁸ | 1.9x10 ⁸ | 3.4x10 ⁸ |

FIGURE CAPTIONS

Fig. 1 Schematic diagram of the biofilm reactor system.

Fig. 2 Width and length dimensions of cell clusters grown in laminar (circles) and turbulent (triangles) flow on days nine (closed symbols) and 23 (open symbols) from Run 1. The clusters grown in the turbulent flow were larger than those in the laminar flow cell and became increasingly elongated over time.

Fig. 3 After 22 days the biofilm grown in laminar flow (A) consisted of cell clusters (C) separated by interstitial voids (Run 1). The biofilm grown in turbulent flow (B) had elongated streamers (S) and patches of ripples (R). Shadow haze is from biofilm growing on the bottom of the flow cell. Flow was from left to right. Scale bars = 500 μm .

Fig. 4 Influence of flow velocity on cell cluster shape in the laminar (●) and turbulent (▼) flow cells over time illustrated by the l:w ratio of the cell clusters for Run 1. Bars indicate one SE, n is indicated above the data points.

Fig. 5 Influence of flow velocity on biofilm surface coverage in the laminar (●) and turbulent (▼) flow cells over time for Run 1. Bars indicate one SE, n = five fields.

Fig. 6 Concentration of the consortia species, *P. aeruginosa* (O), *P. fluorescens* (▽), *K. pneumoniae* (▲), and *S. maltophilia* (■), in the reactor effluent over time for Run 2. The influent glucose nutrient concentration (ppm) is indicated at the bottom of the graph. Bars indicate one SE from triplicate plate counts.

Fig. 7 Change in cell cluster thickness (●) and surface coverage (▼) of biofilm grown in turbulent flow from Run 2. Bars indicate one SE, data points are averaged from a minimum of five measurements. The influent glucose nutrient concentration (ppm) is indicated at the top of the graph. The thickness of the clusters grown in the turbulent flow cell from Run 1 are also shown (O) for comparison.

Fig. 8 Biofilm grown in turbulent flow (Run 2) at: A; 21 days grown on low nutrient media (scale bar = 500 μm), B; same field of view as panel “A” ten hours after switching to high nutrient media, C; day 26, after five days at high nutrient media (scale bar = 100 μm), and D; same field of view as panel “C” at day 28, 2 days after switching back to low nutrient media. Streamers (S) and ripple patches are indicated (R), flow was from left to right.

Fig. 9 Two dimensional nutrient concentration - flow velocity habitat domain diagram based on observational and hypothetical considerations of mass transfer and shear on biofilm morphotypes. The “no growth” region assumes that some minimum nutrient concentration is required for growth and that there is a shear at which no cells can

remain attached. Neither of these assumptions has been demonstrated. It is interesting to note that by moving diagonally across the diagram from top left to bottom right, for a given reactor geometry, various morphotypes may occur while the nutrient loading rate remains constant.

FIGURES

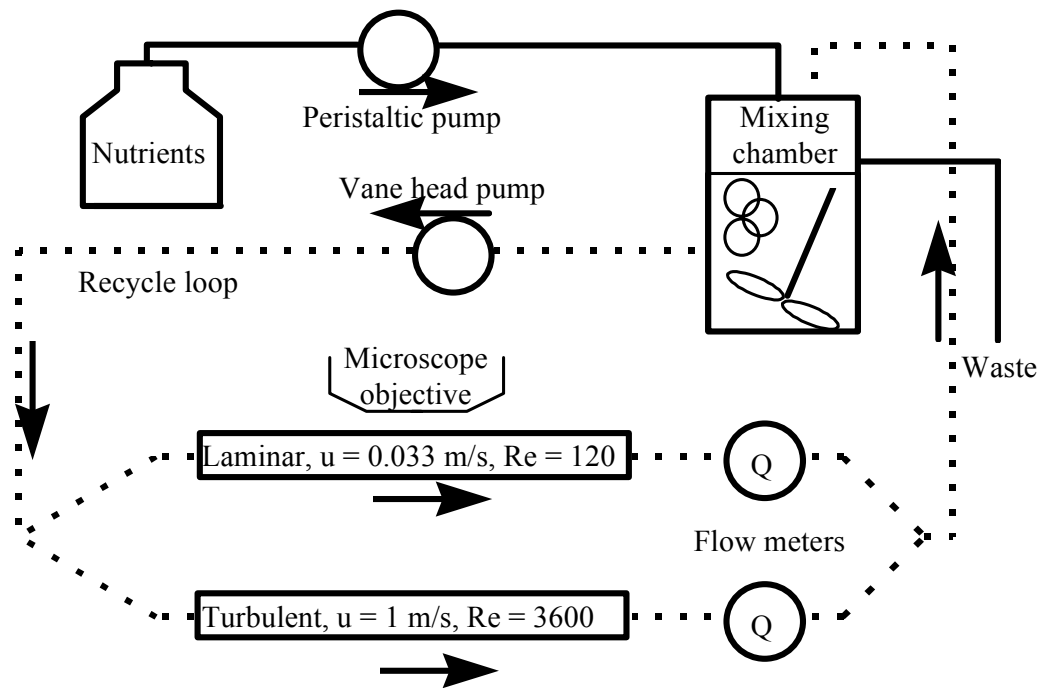


Fig.1

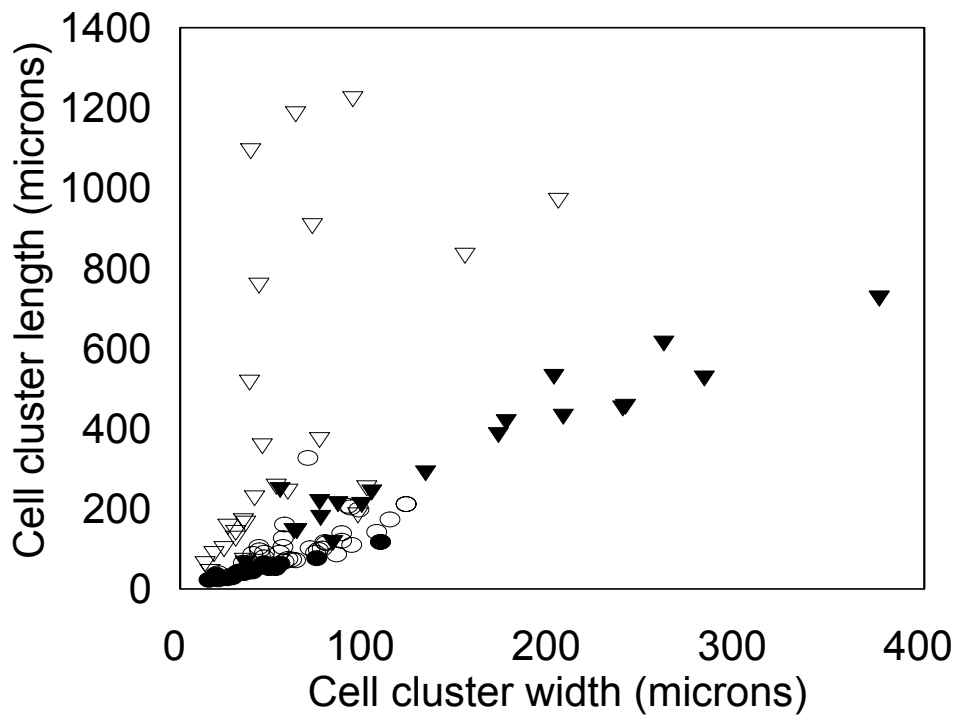


Fig. 2.

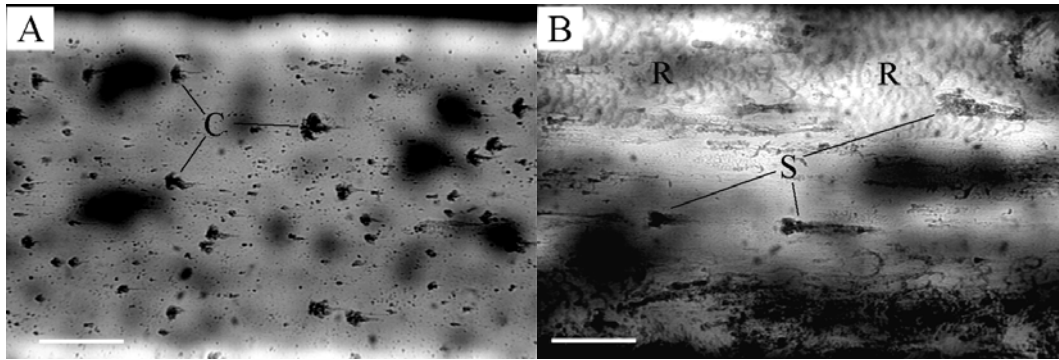


Fig. 3.

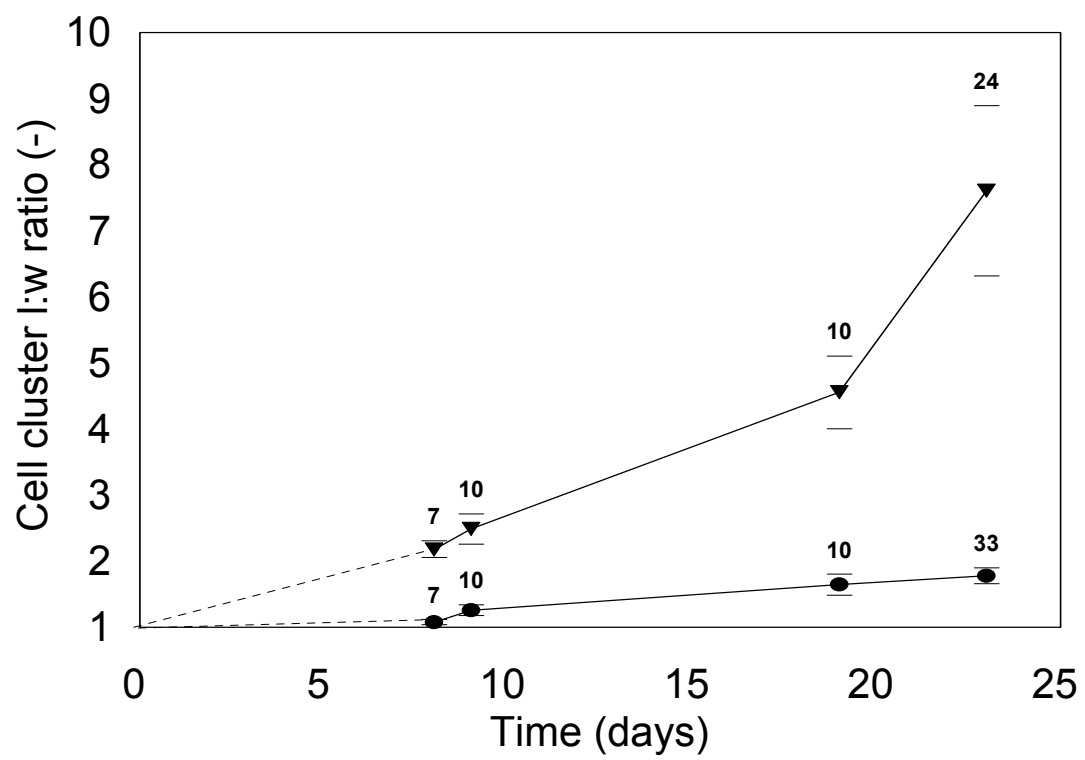


Fig. 4.

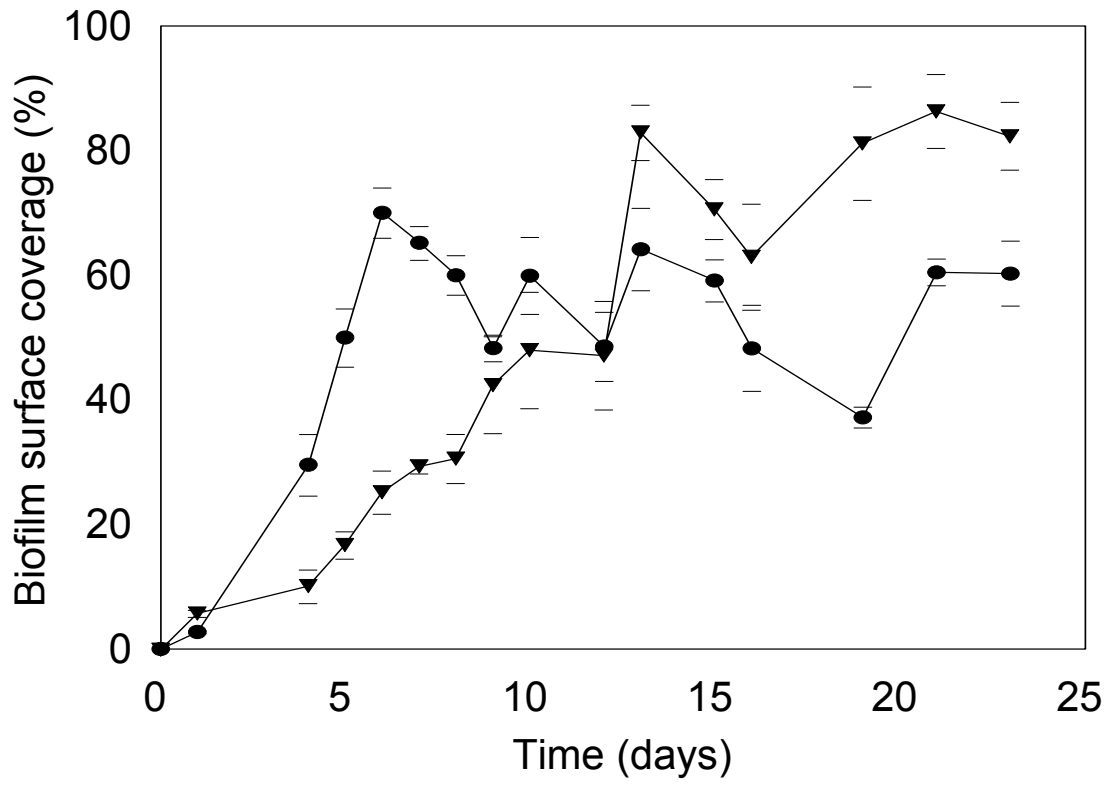


Fig. 5.

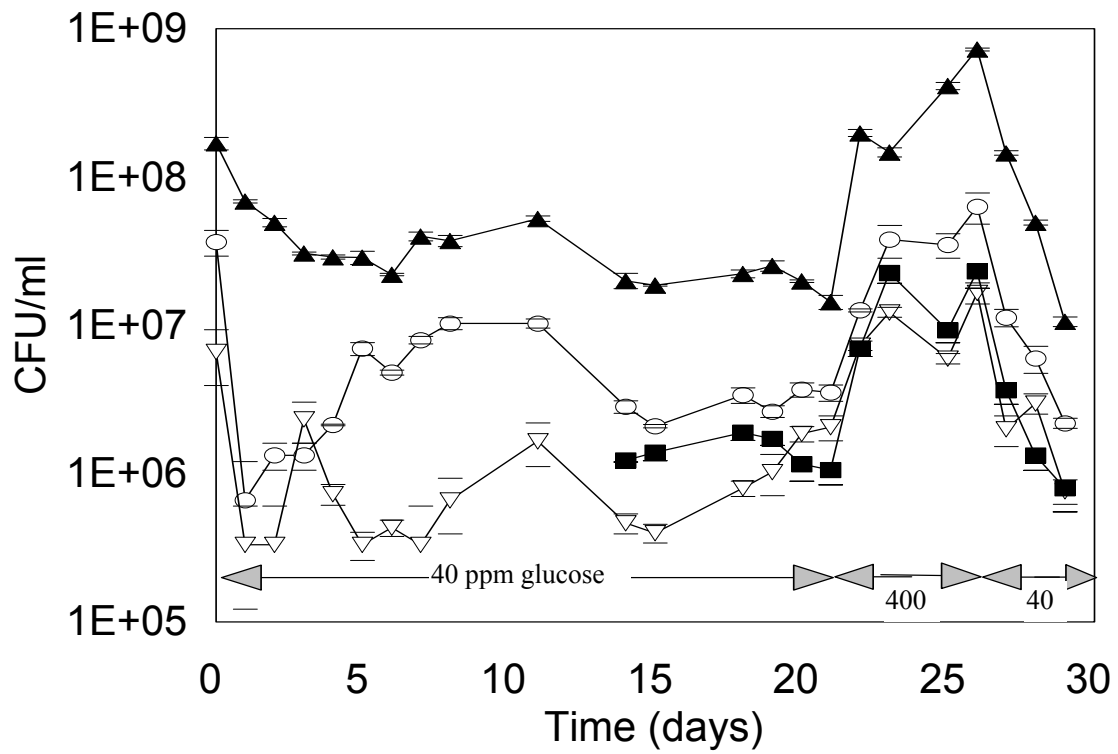


Fig. 6.

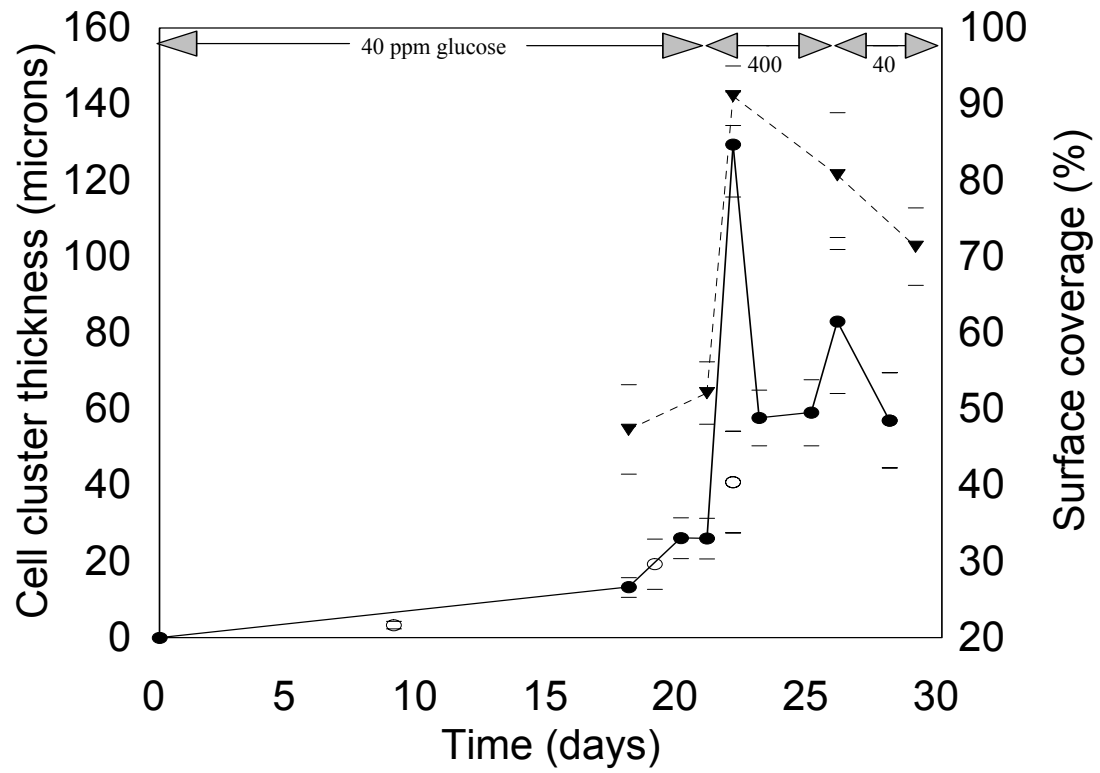


Fig. 7.

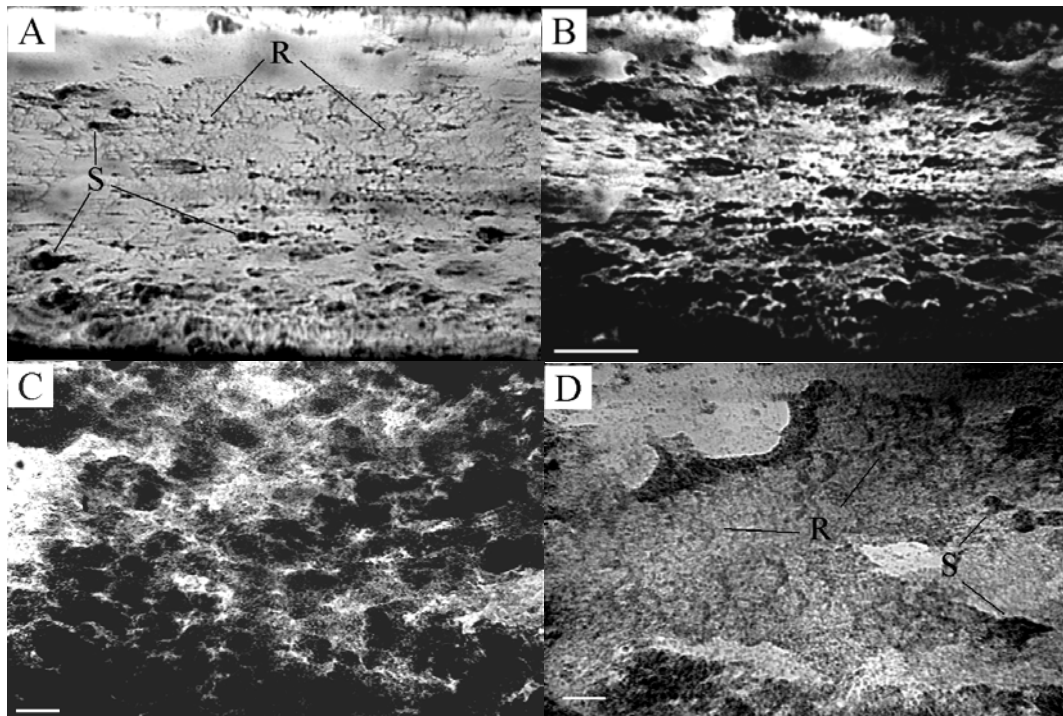


Fig. 8.

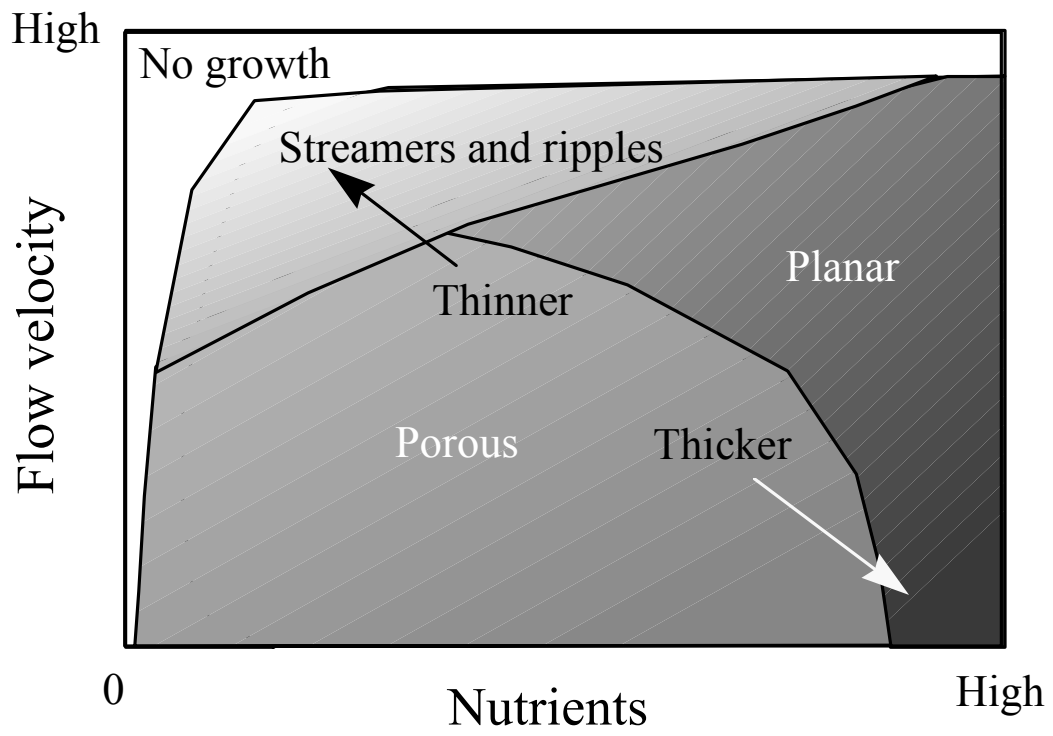


Fig. 9.